World Academy of Science, Engineering and Technology
International Journal of Bioengineering and Life Sciences
Vol:7, No:12, 2013

Development of Scratching Monitoring System Based On Mathematical Model of Unconstrained Bed Sensing Method

Takuya Sumi, Syoko Nukaya, Takashi Kaburagi, Hiroshi Tanaka, Kajiro Watanabe, Yosuke Kurihara

***Abstract*—**We propose an unconstrained measurement system for scratching motion based on mathematical model of unconstrained bed sensing method which could measure the bed vibrations due to the motion of the person on the bed. In this paper, we construct mathematical model of the unconstrained bed monitoring system; and we apply the unconstrained bed sensing method to the system for detecting scratching motion. The proposed sensors are placed under the three bed feet. When the person is lying on the bed, the output signals from the sensors are proportional to the magnitude of the vibration due to the scratching motion. Hence, we could detect the subject's scratching motion from the output signals from ceramic sensors. We evaluated two scratching motions using the proposed system in the validity experiment as follows: 1st experiment is the subject's scratching the right side cheek with his right hand, and; 2nd experiment is the subject's scratching the shin with another foot. As the results of the experiment, we recognized the scratching signals that enable the determination when the scratching occurred. Furthermore, the difference among the amplitudes of the output signals enabled us to estimate where the subject scratched.

***Keywords*—**Unconstrained bed sensing method, scratching, body movement, itchy, piezoceramics.

I. Introduction

FEELING itchy can be occurred as a symptom of various skin diseases affecting patients, who scratch the itchy parts to decrease the itch. Skin inflammation, however, can become worse from the scratching [1] and the patients hardly to sleep well. The gravity of skin diseases accompanied by itching is related to the frequency of the itch [2]. So the more severe the disease is, the longer the scratching time by the patient. The scratching time information is compiled into an index referred to as TST%, which is the ratio of total scratching time (TST) to total measurement time during sleep. The data is correlated to the degree of pruritus in skin diseases such as atopic dermatitis [3], [4]. Therefore, measurement of the scratching is effective in diagnosing skin diseases. Moreover, since the itch occurs irregularly, the patient unconsciously scratches while sleeping. Since patients can control the scratching while they are awake, a more accurate evaluation would be made by monitoring the scratching motion while they are asleep. In clinical practice, an infrared video camera is generally used to monitor the location, pattern, and frequency of scratching during sleep. Using camera, however, is not suitable for daily monitoring, since it infringes on the patients' privacy and it also requires a large-scale system.

Given these circumstances, various smaller-scale methods have been proposed for evaluating scratching motion during sleep. For the most part, they are aimed at recording the motion or the sound of scratching, or the acceleration of wrist movement and its angular velocity. An electromyograph can be used to measure the electrical activity of the muscles in the forearm. Other devices can be used to measure the change in pressure at the back of the hand, the expansion and contraction motions of the finger [1]-[12]. Furthermore, RF-ID can be used to measure limbs' monitoring in sleep diseases [13]. These methods, however, are somewhat bothersome as the sensors must be attached directly to the patient's arms or feet.

One of the effective approaches for daily biosignals monitoring is measuring patients' biosignals without having to wear any sensors on their body. So, in this paper, we describe an unconstrained measurement system for scratching motion based on mathematical model of unconstrained bed sensing method. Furthermore, proposed system can estimate where subject scratch during sleep.

II. Mathematical Model of Unconstrained Bed Sensing Method for Scratching Monitoring System

A. System of Unconstrained Bed Sensing Method

Fig. 1 shows the proposed unconstrained bed sensor system by piezoceramics. The piezoceramics bonded to stainless steel plates are set beneath each of the three feet of the bed to prop the weight of the bed including the person on it. Since piezoceramics have capacitive characteristics, the output voltage in the steady state is zero-biased and changes from zero voltage.

Takuya. Sumi is with the Graduate School of Hosei University, 3-7-2 Kajinocho Koganei-shi, Tokyo 184-8584, Japan.

Shoko. Nukaya is with the Division of Advanced Therapeutical Sciences Tokyo Medical and Dental University, 1-5-45 Yushima, Bunkyo-city, Tokyo 113-8510, Japan (e-mail: nukaya@bioinfo.tmd.ac.jp).

T. Kaburagi is with the Dept. of Industrial and System Engineering, College of Science and Technology, Aoyama Gakuin University, 5-10-1 Fuchinobe, Chuo-ku, Sagamihara-shi, Kanagawa 252-5258, Japan

H. Tanaka is with the University Center for Information Medicine Tokyo Medical and Dental University, 1-5-45 Yushima, Bunkyo-city, Tokyo 113-8510, Japan.

Kajiro. Watanabe is with the System Control Engineering Department, Faculty of Engineering, Hosei University, 3-7-2 Kajinocho Koganei-shi, Tokyo 184-8584, Japan.

Y. Kurihara is with the Dept. of Industrial and System Engineering, College of Science and Technology, Aoyama Gakuin University, 5-10-1 Fuchinobe, Chuo-ku, Sagamihara-shi, Kanagawa 252-5258, Japan (corresponding author to provide phone:+81-42-759-6371; e-mail:kurihara@ise.aoyama.ac.jp).

We defined the variables and constants for the piezoceramics and the unconstrained bed sensing system shown in Fig. 1 as follows:

[Piezoceramics]

A [C/m] or [N/V]	:force part of the piezoceramic device
M [kg]	:mass of bed including person on it
k [N/m]	:stiffness constant of the metal stainless steel plate
d [Ns/m]	:damping coefficient of the metal plate
C [F]	:capacitance between the piezoceramic
R [Ω]	:input resistance of the processor
t [s]	:time
$x(t)$ [m]	:resultant displacement of stainless steel plate
$f(t)$ [N]	:force generated by the devices
$q_i(t)$ [C]	:electric charge generated by external strain or bend to the ceramics
$q(t)$ [C]	:resultant electric charge in the ceramics
$x_{hr}(t)$, $x_{hl}(t)$, $x_{fl}(t)$ [m]	:displacement of device plate set at the head and right corner, head and left corner, and foot and left corner, respectively
$e_{hr}(t)$, $e_{hl}(t)$, $e_{fl}(t)$ [V]	:output voltage due to $x_{hr}(t)$, $x_{hl}(t)$, $x_{fl}(t)$, respectively
$P_{fh}(t)$ [Vs]	:integrated value of the difference of $e_{fl}(t) - e_{hl}(t)$
$P_{rl}(t)$ [Vs]	:integrated value of the difference of $e_{hr}(t) - e_{hl}(t)$

[Bed]

G, G'	:center of gravity (CG)
$F_H(t)$[N]	:forces pushing the bed by heartbeat
$F_R(t)$[N]	:forces pushing the bed by respiration motion
g [m/s^2]	:magnitude of acceleration due to gravity
M [kg]	:weight of the bed with a person on it
L [m]	:length of the bed
L_f [m]	:length from CG to foot side of the bed
L_h [m]	:length from CG to head side of the bed
W [m]	:width of the bed
W_l [m]	:length from CG to left side of the bed
W_r [m]	:length from CG to right side bed of the bed
$l(t)$ [m]	:displacement of CG of the bed from the head to foot direction due to change in position of person on the bed
$w(t)$ [m]	:displacement of CG of the bed from the left to right direction due to change in position of person on the bed
d_H [m]	:distance from the heart to CG
d_R [m]	:distance from the diaphragm for respiration to CG
$\theta_{fh}(t)$, $\theta_{rl}(t)$	:sinking angle of the bed from the head to foot direction and from the left to right direction, respectively

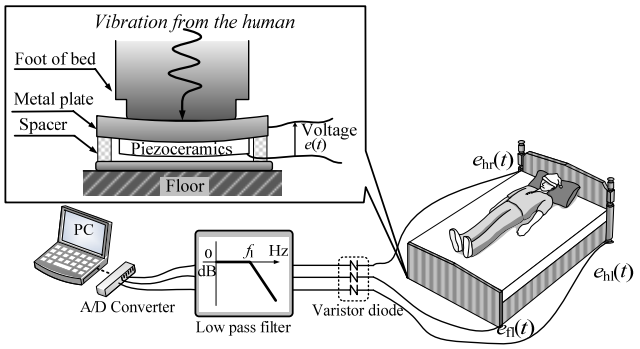

Fig. 1 Bed sensor method using piezoceramics

From the system shown in Fig. 1, we measured the heartbeat and respiration from output $e_{hr}(t)$, $e_{hl}(t)$ or $e_{fl}(t)$. Furthermore, in order to detect changes in position and scratching motions, we integrated the difference between two outputs $e_{hl}(t)$, $e_{fl}(t)$ from the left side and $e_{hl}(t)$, $e_{hr}(t)$ as follows:

$$P_{fh}(t) = \int_o^t \{e_{fl}(\tau) - e_{hl}(\tau)\} d\tau$$
$$P_{rl}(t) = \int_o^t \{e_{hr}(\tau) - e_{hl}(\tau)\} d\tau \quad (1)$$

B. Theoretical Model of the System

Here, we describe mathematical model of unconstrained bed sensing method shown in Fig. 1. Fig. 2 shows a situation where a person is lying on the bed. The location of the heart is at distance d_H from the CG and the diaphragm for respiration is at distance d_R from the CG. The heartbeat and respiration motions push the bed via forces $F_H(t)$ and $F_R(t)$ at these positions, respectively. Furthermore, the person moves toward the foot side of the bed as well as toward the right side of the bed and the CG shifts from G to G' for displacement $l(t)$ and $w(t)$, and the foot side sinks at angle $\theta_{fh}(t)$ and the right side sinks at angle $\theta_{rl}(t)$, respectively, as shown in Fig. 2.

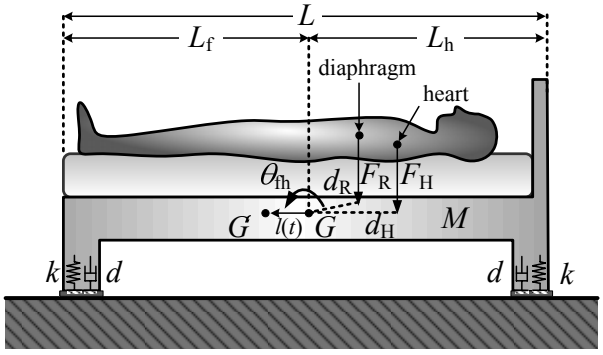

(a) Side view

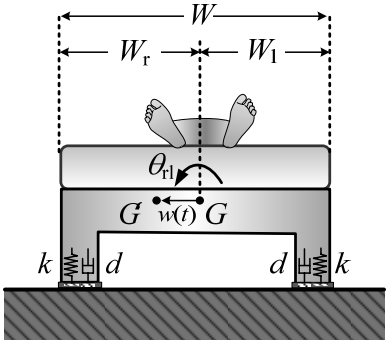

(b) Sole side view

Fig. 2 Model of bed

First, we considered the bed motion and piezoceramic output from the foot and head side. Suppose the shift $l(t)$ is very short and $l(t) << L, L_f, L_h$, thus the sinking angle $\theta_{fh}(t)$ around G and G' is the same. Assuming uniform mass for the bed with a person on it, the inertia moment I_{fh} of the bed around the CG is given by the bed size and weight, then the damping and spring for rotary motion of the bed are as follows:

$$\begin{aligned} I_{fh} &= M\cdot\frac{L_f - l}{3L}\cdot(L_f - l)^2 + M\cdot\frac{L_h + l}{3L}\cdot(L_h + l)^2 \cong \frac{M}{3L}\left(L_f^3 + L_h^3\right) \\ D_{fh} &= d\left\{(L_f - l)^2 + (L_h + l)^2\right\} \cong d\left(L_f{}^2 + L_h{}^2\right) \\ K_{fh} &= k\left\{(L_f - l)^2 + (L_h + l)^2\right\} \cong k\left(L_f{}^2 + L_h{}^2\right) \end{aligned} \quad (2)$$

The rotary motion around G or G' from a steady state condition is then given by:

$$I_{fh}\frac{d^2\theta_{fh}(t)}{dt^2} + D_{fh}\frac{d\theta_{fh}(t)}{dt} + K_{fh}\theta_{fh}(t) = Mgl(t) + d_H F_H(t) + d_R F_R(t) + Lf(t) \quad (3)$$

The displacement of the stainless steel plate of the piezoceramic devices at the foot and head side are given as follows:

$$\begin{aligned} x_f(t) &= (L_f - l)\theta_{fh}(t) \cong L_f\theta_{fh}(t) \\ x_h(t) &= -(L_h + l)\theta_{fh}(t) \cong -L_h\theta_{fh}(t) \end{aligned} \quad (4)$$

The displacement drives the piezoceramic devices with reversible characteristics between static and electrostatic as follows:

$$\begin{aligned} q_i(t) &= Ax_f(t) = AL_f\theta_{fh}(t) \\ R\frac{dq(t)}{dt} + \frac{1}{C}q(t) &= \frac{1}{C}q_i(t) \\ e_f(t) &= R\frac{dq(t)}{dt} \\ f(t) &= -Ae_f(t) \end{aligned} \quad (5)$$

The transfer functions are defined as follows:

$$G_1(s) = \frac{A}{C},\quad G_2(s) = \frac{sCR}{1+sCR},\quad G_3(s\mid L_f) = \frac{\frac{L_f}{I_{fh}}}{s^2 + \frac{D}{I_{fh}}s + \frac{1}{I_{fh}}\left\{K_{fh} + \frac{sRLL_fA^2}{(1+sCR)}\right\}} \quad (6)$$

Then, output e_f with respect to input forces $Mgl + d_H F_H + d_R F_R$ is given:

$$e_f = G_1(s)\cdot G_2(s)\cdot G_3(s\mid L_f)\left(Mgl + d_H F_H + d_R F_R\right) \quad (7)$$

Similarly, from (4) and (7), the output voltage from the head side is given by:

$$e_h = -G_1(s)\cdot G_2(s)\cdot G_3(s\mid L_h)\left(Mgl + d_H F_H + d_R F_R\right) \quad (8)$$

These outputs correspond to the outputs of $e_{hl}(t)$, $e_{hr}(t)$ and $e_{fl}(t)$ in Fig. 1.

C. Measurement of Heartbeat, Respiration and Body Movement

Since we could select a large input resistance R such as 1 to 10 MΩ, which is usual, the cut-off frequency $\frac{1}{2\pi CR}$ of $G_2(s)$ is sufficiently lower than the frequency range of the fundamental and higher components of the heartbeat. Furthermore, we could also select a resonance frequency

$$f = \frac{1}{2\pi}\sqrt{\frac{K_{fh} + (LL_fA^2/R)}{I_{fh}}} = \frac{1}{2\pi}\sqrt{\frac{3Lk\left(L_f^2 + L_h^2\right)}{M\left(L_f^3 + L_h^3\right)}} \quad (9)$$

of the transfer function $G_3(s)$ around the components of the heartbeat, so that output voltages $e_f(t)$ and $e_h(t)$ include the enhanced heartbeat signals. For the low-frequency range where $f < \frac{1}{2\pi CR}$, from (2), (6), (7) and (8) in the time domain, we obtained the following approximations:

$$\begin{aligned} e_f(t) &= AR\frac{L_f}{k(L_f^2 + L_h^2)}\frac{d}{dt}\left\{Mgl(t) + d_H F_H(t) + d_R F_R(t)\right\} \\ e_h(t) &= -AR\frac{L_h}{k(L_f^2 + L_h^2)}\frac{d}{dt}\left\{Mgl(t) + d_H F_H(t) + d_R F_R(t)\right\} \end{aligned} \quad (10)$$

Similarly, output voltages $e_l(t)$ and $e_r(t)$ due to shifting of the body to the left or right side and heartbeat and respiration, can be obtained as follows:

$$\begin{aligned} e_r(t) &= AR\frac{W_r}{k(W_r^2 + W_l^2)}\frac{d}{dt}\left\{Mgw(t) + d_H F_H(t) + d_R F_R(t)\right\} \\ e_l(t) &= -AR\frac{W_l}{k(W_r^2 + W_l^2)}\frac{d}{dt}\left\{Mgw(t) + d_H F_H(t) + d_R F_R(t)\right\} \end{aligned} \quad (11)$$

Thus, (12) can be derived:

$$P_{\mathrm{fh}}(t)=\int_o^t\{e_{\mathrm{fl}}(\tau)-e_{\mathrm{hl}}(\tau)\}d\tau=AR\frac{L}{k(L_{\mathrm{f}}^2+L_{\mathrm{h}}^2)}\{Mgl(t)+d_{\mathrm{H}}F_{\mathrm{H}}(t)+d_{\mathrm{R}}F_{\mathrm{R}}(t)\}$$
$$P_{\mathrm{rl}}(t)=\int_o^t\{e_{\mathrm{hr}}(\tau)-e_{\mathrm{hl}}(\tau)\}d\tau=AR\frac{W}{k(W_{\mathrm{r}}^2+W_{\mathrm{l}}^2)}\{Mgw(t)+d_{\mathrm{H}}F_{\mathrm{H}}(t)+d_{\mathrm{R}}F_{\mathrm{R}}(t)\} \quad (12)$$

when body movements occur, because

$$Mgl(t)>>d_{\mathrm{H}}F_{\mathrm{H}}(t)+d_{\mathrm{R}}F_{\mathrm{R}}(t)$$

and

$$Mgw(t)>>d_{\mathrm{H}}F_{\mathrm{H}}(t)+d_{\mathrm{R}}F_{\mathrm{R}}(t)$$

(12) can simply be rewritten as:

$$P_{\mathrm{fh}}(t)=\frac{ARLMg}{k(L_{\mathrm{f}}^2+L_{\mathrm{h}}^2)}l(t)$$
$$P_{\mathrm{rl}}(t)=\frac{ARWMg}{k(W_{\mathrm{r}}^2+W_{\mathrm{l}}^2)}w(t) \quad (13)$$

where each is linearly proportional to the shift in the CG at the foot to the head side and at the left to the right side, from which we can estimate the movement of the person on the bed.

III. Validity Experiment

A. Experimental Settings

Fig. 3 shows the experimental system and structure of piezoceramic sensor used for the proposed unconstrained bed sensing system. The ceramics in this sensor is 20mm in diameter and is firmly affixed to a brass metal plate, which is 25mm in diameter. This device is typically used for a buzzer. The device is bonded to a stainless steel plate of 1mm in thickness and 50mm in diameter. Under the stainless steel plate is a washer with an inner radius of 15mm, outer radius of 25mm, and thickness of 2mm. The bottom is covered with an aluminum plate that is the same size as the stainless steel plate.

The sensor has the following characteristics: 1×10^{-3} C/m, which is the displacement of electrical charge by piezoelectricity. The capacitance is 0.01μF. Due to the capacitive characteristics of piezoceramics, the output voltage in the steady state is zero-biased and changes from zero voltage. The bed used in Fig. 4 is a coil cushion type weighing 60kg and measuring 1.0×2.1 m. Three piezoceramic sensors are placed under the three legs of the bed. The outputs $e_{\mathrm{hr}}(t)$, $e_{\mathrm{hl}}(t)$ and $e_{\mathrm{fl}}(t)$ measured using the piezoceramic sensors go through the low-pass filter to remove the high-frequency noise component. The cutoff frequency fl of the low-pass filter is set to 12 Hz.

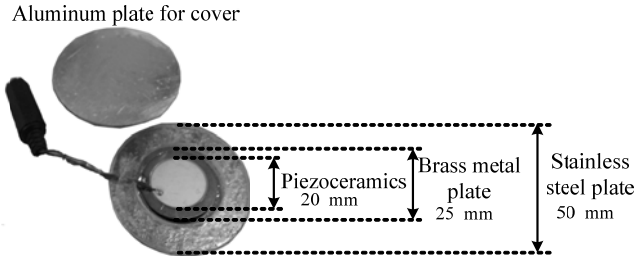

Fig. 3 Inner structure of a piezoceramics sensor

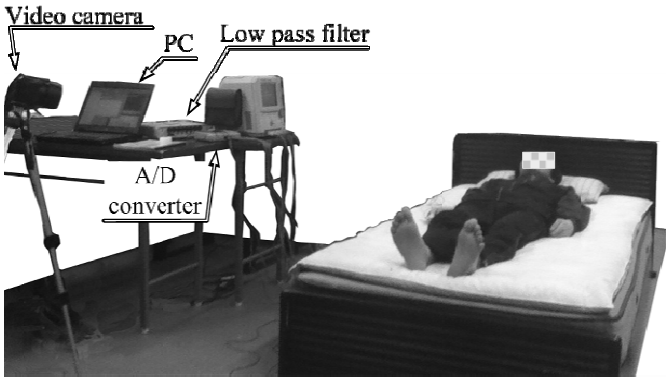

Fig. 4 Experimental system

The output signals from the low-pass filters are A/D-converted, in which the sampling interval is set to 1 ms and the scale range to ±1 V using a data logger (NR-2000, Keyence Co. Ltd.). The subject in this experiment was male, approximately 172cm in height and 63kg in weight, and did not suffer from any sleep disorders.

B. Experimental Procedures

As the starting position, the subject is lying on back at the center of the bed with the arms and legs straight, as shown in Fig. 4. The subject scratches two cases as follows.

(1st Experiment)

The subject scratches his cheek 20 times. He then returns the arm back to the starting position. After a 5sec. pause, the subject once again scratches his cheek 20 times in a row. The set of scratching motions is repeated 35 times.

(2nd Experiment)

The subject scratches his left shin 10 times by his right foot. He then returns his right foot back to the starting position. After a 5sec. pause, the subject once again scratches his left shin 10 times in a row. The set of scratching motions is repeated 5 times. Similarly, subject scratches his right shin 10 times by left foot. And subject repeated the scratching motion 5 times.

Since scratching is a reciprocating motion of the fingers, the sensor extracts the cyclically changing periods as scratching time in its data output.

IV. Experimental Results

A. Results of 1st Experiment

Fig. 5 shows the results of one period of scratching of right cheek. From top to bottom in the Fig. 5 (a) shows $e_{hl}(t)$, $e_{hr}(t)$, $e_{fl}(t)$ and in Fig. 5 (b) shows $P_{fh}(t)$ and $P_{rl}(t)$.

The subject scratched his cheek from about 4 s to 7.5s. At the beginning and end, from about 3 to 4s and 7.5 to 9s, the subject had being moved his right arm, which occurred a large change in the output from all sources. When the subject was resting quietly, the output signal from piezoceramic was hardly changed. While scratching motion, all sensors show a cyclic change in signal simultaneously.

From 0 to 3s in Fig. 5 (a), because the subject's hand is stationary beside his body, The sensors $e_{hl}(t)$, $e_{hr}(t)$ and $e_{fl}(t)$, therefore measure the heartbeat signal. The waveform from 3 to 4s corresponds to the hand moving toward the cheek on the face. The wave shape from 4 to 7.5s corresponds to the 20 times of scratching motion, and $e_{hl}(t)$, $e_{hr}(t)$ and $e_{fl}(t)$ is synchronized with the scratching motion and shows large cyclical fluctuations. The comparison among $e_{hl}(t)$, $e_{hr}(t)$ and $e_{fl}(t)$ shows that the outputs from $e_{hl}(t)$ and $e_{hr}(t)$, which are closer to the head, have a larger-amplitude wave shape than those from $e_{fl}(t)$, which are closer to the feet. Moreover, the output from $e_{hr}(t)$, which is positioned beneath the right side of the head, becomes the largest among the three, since the subject scratches his right cheek. Therefore, the more distant the piezoceramics sensors are from the scratching point, the smaller their output signals are. The wave shape between 7.5 and 9s corresponds to the hand motion retuning to the original position. During this period, rather smooth fluctuations appear, similar to that during the period between 3 and 4s. Between 9 and 12s, the subject's hand once again becomes stationary beside his body, and the heartbeat component is also detected again.

The length of the scratching period can be confirmed as the output signal changes with the scratching motion. When the subject's hand is stationary, both $P_{fh}(t)$ and $P_{rl}(t)$ fluctuated slightly centering around 0. Both $P_{fh}(t)$ and $P_{rl}(t)$ largely changed due to the arm motion, and slightly fluctuated in the minus area during the scratching motions. The $P_{fh}(t)$ change toward the minus means the subject's center of gravity shifted toward the pillow, and the $P_{rl}(t)$ change toward the minus means the center of gravity shifted toward left: These gravity changes correspond to the motion of the subject's arm.

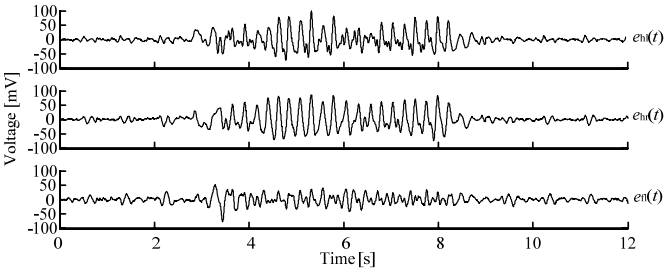

(a) The outputs of piezoceramic sensors

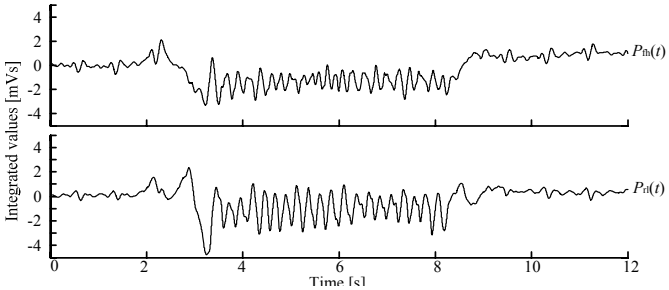

(b) The integrated values of the outputs

Fig. 5 Results of the scratching motion of right cheek by right hand

B. Result of 2nd Experiment

Fig. 6 shows the results of one period of scratching of the left side shin by right foot. From top to bottom in the Fig. 6 (a) shows $e_{hl}(t)$, $e_{hr}(t)$, $e_{fl}(t)$ and in Fig. 6 (b) shows $P_{fh}(t)$ and $P_{rl}(t)$.

As with the scratching motion above, cyclical output signals corresponding to the feet movements can be confirmed. When the feet move, the outputs from the sensors near the feet become larger than those from the ones near the pillow. The integral results showed the amplitude of $P_{fh}(t)$ was larger than that of $P_{rl}(t)$. Since the scratching motion of the foot is in the head-foot direction, the output of $P_{fh}(t)$ largely changed corresponding with the motion. As there was little movement toward right or left, there was little change in $P_{rl}(t)$ due to the transfer of the center of gravity, either.

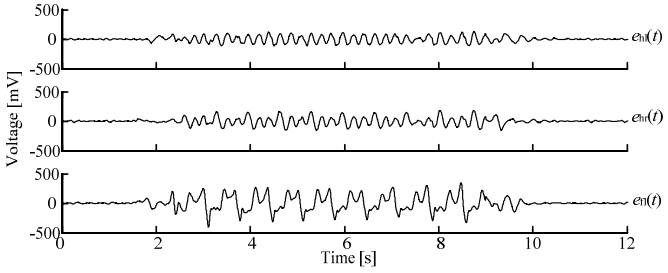

(a) The outputs of piezoceramic sensors

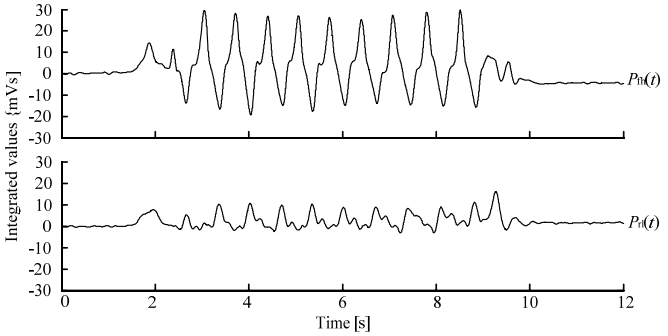

(b) The integrated values of the outputs

Fig. 6 Results of the scratch motion of the left shin by right foot

V. Discussion

The measurement results from the scratching motions all showed cyclical signals with relatively large amplitude, which

enables the measurement of the length of the scratching motions. The length of the scratching motion is correlated with the gravity of the skin disorders, and its index, TST%, can be obtained as shown below.

Let the total measurement time and the total scratching time be T_m and T_s respectively. The TST% is calculated as follows:

$$TST\% = \frac{T_S}{T_m} \times 100$$

This enables the unconstrained measurement and evaluation of the scratching motions while the patients are asleep.

The sensors are set beneath the bed, so there is less awareness of their presence compared to conventional bed sensing and scratching monitoring systems [1]-[12].

In the case of skin diseases characterized by itching, this method enables contact-free measurement of scratching frequency during sleep, which is normally very difficult to ascertain. This system can measure the period of scratching motion, and calculate the TST% for monitoring and the acquisition of detailed information.

The $P_{fh}(t)$ and $P_{rl}(t)$ in (1) enables the acquisition of the data on the transfer of patient's center of gravity on the bed due to the body movements. The data can be applied to the estimation of the scratched area from the body movement before the scratching.

The positive and negative output of $P_{fh}(t)$ correspond to the head-foot direction and the foot-head direction of the transfer of the center of gravity: The positive and negative output of $P_{rl}(t)$ correspond to the left-right direction and the right-left direction of the transfer of the center of gravity. If the $P_{fh}(t)$ is larger than the $P_{rl}(t)$, the scratching is with a foot; and if not, it is with a hand.

The amplitude of $P_{fh}(t)$ while the foot is in a scratching motion is larger than that of $P_{rl}(t)$, because the output signals from the sensors near the feet are larger than the output signals from those near the pillow. Further enhancing the difference in the amplitude are the facts that: 1) there is little transfer of the center of gravity to the right or the left, and; 2) in (1), $P_{rl}(t)$ only uses the output signals only from the sensors near the pillow for the calculation, while $P_{fh}(t)$ applies the output signals from those near the feet.

As the experiment in 2nd experiment shows, the proposed system not only enables the measurement of the itching through the scratching motions, but can be applied to observe abnormal motions of the limbs such as those accompanying the restless legs syndrome, which can cause insomnia. The proposed system has great advantage in its capability to carry out such measurements without directly touching the sleeping subject.

VI. Conclusions

In this paper, we proposed a novel sensing device using piezoceramic sensors to measure scratching motions based on mathematical model of unconstrained bed sensing method. This device consists of a piezoceramic sandwiched between metal plates and placed under the legs of the bed. This device can measure micro-vibrations produced by the scratching motion of the subject on the bed. The TST%, an important index for evaluating the scratching motions, could be calculated from the signals measured with the ceramic sensor devices. Furthermore, using the integrated value of the difference of output signals from three ceramic sensor devices, a change in position of the person on the bed could be detected.

Acknowledgment

This work was supported by a Grant-in-Aid for Scientific Research (23760372).

References

[1] T. Ebata, et al., "The characteristics of nocturnal scratching in adults with atopic dermatitis", British Journal of Dermatology Vol. 141, pp.82-86, 1999.
[2] T. Ebata, et al., "Use of a wrist activity monitor for the measurement of nocturnal scratching in patients with atopic dermatitis", British Journal of Dermatology Vol. 144, pp.305-309, 2001.
[3] T. Ebata, H. Aizawa, R. Kamide, "An Infrared Video Camera System to Observe Nocturnal Scratching in Atopic Dermatitis Patients," *British Journal of Dermatology* Vol. 23, pp. 155-155, 1996.
[4] H. Izumi, et al., "A Simplified Method for the Measurement of Nocturnal Scratching with an Infrared Video Camera," The Skin Vol. 39, pp. 560-563, 1997.
[5] K. Umeda, et al., "A novel acoustic evaluation system of scratching in mouse dermatitis: Rapid and specific detection of invisibly rapid scratch in an atopic dermatitis model mouse," Life Science Vol. 79, pp. 2144-2150, 2006.
[6] Y. Kawabe. K. Aritake, Y. Noro, K. Umeda, H. Mizutani, "A Study of sensor for Detection of Human Scratching Behavior during Sleep," Tokai of society related to electricity branch union rally O-329, 2007.
[7] M. Konishi, K. Aritake, Y. Noro, K. Umeda, H. Mizutani, "A Study of sensor for Detection of Human Scratching Behavior during Sleep," Tokai of society related to electricity branch union rally O-322, 2008.
[8] H. Yokoi, Y. Noro, K. Umeda, H. Mizutani, "Detection of Human Scratching Behavior during Sleep with Acceleration sensor," Tokai of society related to electricity branch union rally O-323, 2008.
[9] R. Felix, S. Shuster, "A New method for the measurement of itch and the response to treatment," British Journal of Dermatology Vol. 93, pp. 303-312, 1975.
[10] J. A. Savin, W. D. Paterson, I.Oswald, "Scratching during Dleep," The Lancet Vol. August 11, pp. 296-297, 1973.
[11] K. Endo, H, Sumitsuji, T. Fukuzumi, J. Adachi, T. Aoki, "Evaluation of Scratch Movements by a New Scrath-Monitor to Analyze Nocturnal Itching in Atopic Dermatitis," Acta Derm Venereol (Stockh) Vol. 77, pp. 432-435, 1997.
[12] T. Aoki, H. Kushimoto, Y. Hishikawa, J. A. Savin, "Nocturnal scratching and its relationship to the disturbed sleep of itchy subject," Clinical and Experiment Dermatology Vol. 16, pp. 268-272, 1991.
[13] C. Occhiuzzi and G. Marrocco, "The RFID Technology for Neurosciences: Feasibility of Limbs' Monitoring in Sleep Diseases," Information Technology in Biomedicine Vol. 14, No. 1, pp. 37-43, 2010.

Takuya Sumi received the B.E. degrees in system control engineering from Hosei University, Tokyo, Japan, in 2012. Now he belongs to graduated school Hosei. His current interest is bio-sensing method.

Shoko Nukaya received B.E. degree from Waseda University, Tokyo, in 1992. She joined Sony Corporation. For 12 years, as a software engineer, She had been developing consumer mobile products. In 2005, she received M.S. degree from Eastern Michigan University, MI, US. After graduation, she joined Nokia Corporation. Since 2010, she has started the research at Tokyo Medical and Dental University Graduate School as a PhD student. Her major interests are healthcare innovation by utilizing IT.

Takashi Kaburagi was born in 1980. He received his BSEE, ME and Ph.D. degrees from Waseda University, Japan in 2003, 2005, and 2009 respectively. He is an Assistant Professor at the Department of Industrial and Systems

Engineering, Aoyama Gakuin University. His current research interests are time-series data analysis, bioinformatics, and information efficient text input systems.

Hiroshi Tanaka received D.M. and Ph.D. degrees from the University of Tokyo, in 1981 and 1983, respectively. From 1982, he served as a lecture at University of Tokyo; from 1987, as an Assistant Professor at Hamamatsu University School of Medicine; from 1991 to present, as a Professor at Department of Medical informatics Tokyo Medical and Dental University. From 1995, he is a Director General at University Center for Information Medicine Tokyo Medical and Dental University. From 2006, he is a Director of Biomedical Science PhD Program, the Chief Manager and President of the JAMI, and Chairperson of the JHITI.

Kajiro Watanabe received the M.E. and Ph.D. degrees from the Tokyo Institute of Technology, in 1968 and 1971, respectively. From 1969 to 1971, he served as a Research Assistant at Faculty of Engineering Hosei University. From 1971, he served the Lecture; from 1974 to 1984, as an Assistant Professor; and from 1985 to present, as the Professor. From 1980 to 1981, he served as the Visiting Associate Professor at Oakland University, Rochester, MI, and from 1981 to 1982 as the Research Associate at the University of Texas, Austin. In the industrial filed, he acts as an authorized C.E. He is Chief Researcher of the several projects conducted by the Ministry of Economy, Trade, and Industry Japan. His major interest is the control and instrument and he is currently interested in bio-measurement, sports measurement, robotics, fault diagnosis, vehicle, environmental monitoring, and intelligent control. He holds 75 patents, has 15 publications in the control engineering field and more than 332 referenced journals and conference proceedings. Dr. Watanabe is a member of the Society of Instrument and Control Engineers.

Yosuke Kurihara received M.E. and Ph.D. degrees from Hosei University, Tokyo, in 2003 and 2009, respectively. He joined Hitachi Software Engineering Ltd. in 2003. From 2009 to 2013, he served as Assistant Professor at Seikei University. From 2013 to the present, he has served as Associate Professor at Aoyama Gakuin University. His research interests include system engineering, sensing methods, bio-sensing, and system information engineering. He is a member of the Japanese Society for Medical and Biological Engineering.